Study of magnetic hysteresis effects in a storage ring using precision tune measurement *

Wei Li(李为)[1,2;1)] Hao Hao[2] Stepan F. Mikhailov[2] Wei Xu(徐卫)[1] Jing-Yi Li(李京祎)[1]
Wei-Min Li(李为民)[1] Ying. K. Wu[2;2)]

[1] National Synchrotron Radiation Laboratory, University of Science and Technology of China, Hefei 230029, China
[2] Triangle University Nuclear Laboratory/Physics Department, Duke University, Durham 27705, USA

Abstract: With the advances in accelerator science and technology in recent decades, the accelerator community has focused on the development of next-generation light sources, for example diffraction-limited storage rings (DLSRs), which require precision control of the electron beam energy and betatron tunes. This work is aimed at understanding magnet hysteresis effects on the electron beam energy and lattice focusing in circular accelerators, and developing new methods to gain better control of these effects. In this paper, we will report our recent experimental study of the magnetic hysteresis effects and their impacts on the Duke storage ring lattice using the transverse feedback based precision tune measurement system. The major magnet hysteresis effects associated with magnet normalization and lattice ramping are carefully studied to determine an effective procedure for lattice preparation while maintaining a high degree of reproducibility of lattice focusing. The local hysteresis effects are also studied by measuring the betatron tune shifts which result from adjusting the setting of a quadrupole. A new technique has been developed to precisely recover the focusing strength of the quadrupole by returning it to a proper setting to overcome the local hysteresis effect.

Keywords: magnetic hysteresis, storage ring, betatron tune, magnet normalization

PACS: 29.20.db, 75.60.Ej **DOI:** 10.1088/1674-1137/40/12/127002

1 Introduction

With the advances in accelerator science and technology in recent decades, next-generation synchrotron radiation sources will be developed with higher brightness, better coherence, and improved beam control and stability. For versatile, multi-user operation, the accelerator community has focused on the development of next-generation light sources based on diffraction-limited storage rings (DLSRs) [1–4]. The development of DLSRs faces a number of scientific and technological challenges in several areas [5–8], including designing and operating ultra-low emittance lattices (typically, tens of picometers) with large enough single-particle nonlinear dynamics, better control of beam parameters and beam instability compared with the third-generation light sources, good beam lifetime with a limited dynamic aperture, etc.

Precision control of the electron beam energy and betatron tunes in the storage ring is critical for next-generation light sources to produce photon beams at exact wavelengths as designed, and to realize good injection efficiency and beam lifetime without losing dynamic aperture due to lattice focusing errors. The improved beam parameter control can also greatly benefit the operation of existing storage ring-based light sources. In recent years, techniques have been developed to improve the stability of the electron beam energy and orbit by precisely controlling the air temperature in the storage ring to the level of 0.1 ℃ [9]. In the last decade, two advanced techniques have been developed to measure the absolute energy of the electron beam in the storage ring with a relative accuracy of a few 10^{-5}. One method uses the Resonant Spin Depolarization (RSD) technique for a high energy electron beam (typically above 1 GeV) [10, 11], and the other uses the Compton scattering technique for a low energy beam (typically a few hundreds of MeV) [12–14]. However, neither technique is readily available to many operational light sources which do not have a means to accurately measure the electron beam energy during routine operation.

Since the 2000s, field-programmable gate array (FPGA) based digital bunch-by-bunch longitudinal and

Received 18 April 2016, Revised 2 July 2016
∗ Supported by National Natural Science Foundation of China (11175180, 11475167) and US DOE (DE-FG02-97ER41033)
1) E-mail: wei.li3@duke.edu
2) E-mail: wu@fel.duke.edu

transverse feedback systems have been widely utilized to mitigate beam instabilities at light source storage rings. The transverse feedback (TFB) has been used to make precision measurements of betatron tunes for beam studies and for user operation. For example, at the Duke FEL laboratory a precision tune measurement system was developed based upon the bunch-by-bunch transverse feedback (TFB) [15]. With this system, the betatron tunes can be accurately measured with an rms uncertainty of a few 10^{-5}, as limited by the short-term stability of magnet power supplies and the maximum data memory available in the TFB system. This new diagnostic capability has made it possible to carry out precision studies of various effects related to the electron beam energy and betatron tunes.

In this work, we report our recent experimental study of the magnetic hysteresis effects and their impact on the electron beam energy and focusing in the storage ring using the TFB based tune measurement system without the need for absolute beam energy measurements. This precision tune measurement system has allowed us to advance beam study in two areas. First, it has enabled us to investigate the magnet hysteresis effect associated with magnet normalization. The new insight from this study has allowed us to experimentally determine the effectiveness of a particular magnet normalization routine, thus providing a way to devise a more efficient magnet normalization procedure. Second, using this system to study the tune changes resulting from adjusting the setting of a quadrupole, we have developed a new technique to return the quadrupole to a proper setting to precisely recover its focusing strength, overcoming the local magnetic hysteresis effect. The main experimental results in these areas will be presented in the following sections.

2 Magnetic hysteresis effects

In this section, we provide a brief review of ferromagnetic hysteresis. Magnetic hysteresis describes the nonlinear response of a ferromagnetic material to the imposed magnetizing field (the H-field), producing hysteresis loops of finite areas when the H-field undergoes repetitive cycles between two fixed values, see Fig. 1. This lack of reproducibility of the material magnetization for a given H-field, a "magnetic memory" effect, is the result of the behaviors of the magnetic domains in the material, as a certain amount of energy is needed to reorient the magnetic domains, and/or change the domain wall boundaries and sizes.

The study of magnetic hysteresis has a long history going back to the late 1800s [16, 17]. Since the mid-1980s, however, hysteresis effects have become a subject of intense research by scientists and engineers from a variety of research areas, which has significantly advanced our understanding of the hysteresis phenomenon in general. Typically, two different approaches are taken. The first is a physics based approach built on a certain statistical-mechanical theory by applying first-order phase transition to analyze various spin systems [18–20]. The second approach uses phenomenological models. Some of the most successful models are the Preisach model [21], Coleman-Hodgdon model [22, 23], and Jilies-Atherton model [24, 25]. The Jiles-Atherton model, developed in the early 1980s, connects the model parameters directly with the physical parameters of the magnetic materials, in particular, the spinning and rotation of the magnetization in these materials [25–27]. This model has also been successfully extended to describe minor hysteresis loops [28].

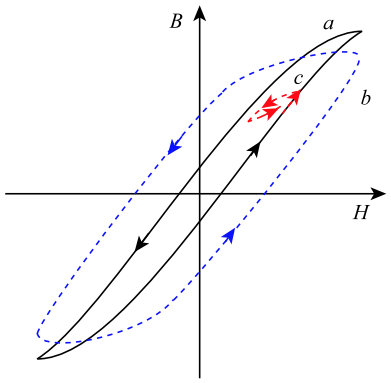

Fig. 1. (color online) Hysteresis loops obtained on a magnetic-curve tracer for soft iron bars. Solid line a: cycle is performed slowly; Blue dash line b: cycle is performed fast. Red dot line c: a minor loop. [18, 31]

The well-known magnetic hysteresis effect is DC hysteresis, which is represented by a quasi-static loop showing the equilibrium position of the bulk material magnetization. Since the 1980s, research has turned to investigate the nonequlibrium behavior of frequency-dependent hysteresis in different types of magnetic materials, including non-conducting materials such as high frequency ferrites [29] and electrically conducting materials [30]. The frequency-dependency studies of conducting materials, such as the soft iron used to construct accelerator magnets, takes into account the eddy current effect. However, it assumes that the magnetic field penetrates uniformly throughout the material [30].

Even with significant advances in modeling and understanding magnetic hysteresis in recent decades, controlling and managing the adverse effects associated with magnetic hysteresis remains a very difficult and challenging task for present and future generation light source storage rings. These challenges are manifest in several areas, including (1) precise and accurate control of the accelerator magnet field with a very small relative uncertainty of 10^{-4} to 10^{-5}; (2) managing magnetic hystere-

sis associated with the skin effect, which can be important for solid-core magnets even at a low field ramping rate; (3) dealing with the interference of the magnetic field from adjacent magnets. In this work, we will report our experimental study of small changes in magnetic fields related to magnetic hysteresis using a precision tune measurement system.

3 Scaling the settings of dipoles and quadrupoles

A typical way to study magnet hysteresis is to determine the relation between the B-field and H-field by measuring the B-H curve [32, 33], where the H-field is produced by the coil current and the B-field is the nonlinear response to the H-field. However, it is impractical to directly measure the H-field and B-field in a well installed facility like the Duke Storage Ring (DSR). Instead, we use the precision betatron tune measurements to study the magnet hysteresis. In this section, we provide a brief view of how dipole and quadrupole magnet field changes can be studied using the measured tune changes.

The generic Hamiltonian of a charged particle in a normal (non-skew) quadrupole, a sextupole, or a combined-function quadru-sextupole under the impulse magnetic field model can be expressed in the Cartesian coordinate system as [34, 35]:

$$H(x,y,\delta,p_x,p_y,l;s)\approx\frac{p_x^2+p_y^2}{2(1+\delta)}+\frac{1}{2}K_1(x^2-y^2)+\frac{1}{3}K_2(x^3-3xy^2), \tag{1}$$

where x, y are transverse displacements from the designed orbits; $p_{x,y}=P_{x,y}/P_0$ are the scaled momenta (canonical to x, y respectively) which are given by scaling the momenta $P_{x,y}$ by the designed momentum P_0; $\delta=(P-P_0)/P_0$ is the scaled momentum deviation with P being the particle's momentum; l is the path length; and s is an independent variable, giving the particle's orbital position along the storage ring. $K_1=\frac{1}{B_0\rho_0}\frac{\partial B_y}{\partial x}|_{x=y=0}$, $K_2=\frac{1}{2!}\frac{1}{B_0\rho_0}\frac{\partial^2 B_y}{\partial x^2}|_{x=y=0}$ are the strengths of the normal quadrupole and sextupole, respectively, and $B_0\rho_0$ is the magnetic rigidity. The related equations of motion in the transverse directions, for example the x-direction, are

$$\begin{cases}\dfrac{\mathrm{d}x}{\mathrm{d}s}=\dfrac{p_x}{1+\delta}\\[2ex]\dfrac{\mathrm{d}p_x}{\mathrm{d}s}=-(K_1x+K_2(x^2-y^2))\end{cases} \tag{2}$$

$$\frac{\mathrm{d}^2x}{\mathrm{d}s^2}+\frac{1}{1+\delta}(K_1x+K_2(x^2-y^2))=0. \tag{3}$$

The linear focusing strength is given by $K_1(s)/(1+\delta)=P_0K_1(s)/P$. Therefore, the betatron tune depends on both the strength of the quadrupoles and the momentum (or energy) of the charged particle. These observations are still valid even if we take into account the weak focusing provided by the dipole magnets.

The momentum of the charged particle can be determined by the integrated magnetic field it sees along its closed orbit. Ignoring the betatron motions (as the average effect is negligible for small amplitude, fast transverse oscillations), the momentum of a relativistic charged particle P is given by

$$P=\frac{1}{2\pi c}\int_{\text{closed-orbit}}qB_y(s)\mathrm{d}s\approx\frac{1}{2\pi c}\int_{\text{dipoles}}qB_y(s)\mathrm{d}s. \tag{4}$$

Hence the momentum P is proportional to the strength of the dipoles. Consequently, for a storage ring, if the strengths of all dipoles and all quadrupoles are changed by the same relative amount, the betatron tunes of the beam will remain the same. This is the basic principle for performing energy ramping in a storage ring or in a booster synchrotron. This observation means that the betatron tunes will be a good measure to determine discrepancies in the magnetic field changes between quadrupoles and dipoles.

The above idea can be tested using a field strength scaling method by measuring the betatron tune changes as the result of proportionally changing only the dipole magnetic field (Method 1), or only the quadrupole magnetic field (Method 2). Method 1 is a commonly used technique to measure the storage ring natural chromaticity in a conventional storage ring with only separate-function magnets and with well-corrected beam orbits in quadrupoles. Changing the magnetic field of all dipoles alone by the same relative amount will cause a change of the electron beam energy without altering the orbit in the quadrupoles and other magnets (such as sextupoles), resulting in a variation of betatron tunes caused only by the change in effective focusing of all quadrupoles. In Method 2, the electron beam energy remains unchanged by keeping the same dipole magnetic field strength. The betatron tunes will vary as the strength of all other magnets (quadrupoles and sextupoles) is changed by the same relative amount. In both methods, we expect that the linear dependency of the betatron tunes on the relative change in the field strength will give the same value, which corresponds to the natural chromaticity for a storage ring with separate-function magnets. In fact, here we are proposing an alternative way to measure the storage ring natural chromaticity using Method 2.

These effects are measured in the DSR by separately scaling the magnetic field strength of all dipoles or all quadrupoles/quadru-sextupoles. As shown in Fig. 2, the betatron tunes show an opposite response in Method 2 compared to Method 1 by comparing subplot Fig. 2 (a) vs (c) for the horizontal tune (ν_x) and Fig. 2 (b) vs (d) for vertical tune (ν_y). The slope of the tune variations gives the measured natural chromaticity. In the horizontal (vertical) direction, the tune slopes are −9.75 (−8.54) by varying dipole fields only, and 9.93 (8.73) by varying quadru-sextupole fields only. The relative difference of 2% between the two different methods (in both directions) is remarkably small, recognizing the fact that the tune stability and accuracy of the tune measurement system are of the order of a few 10^{-5} (absolute values), and that the magnetic field stability and controllability is of the order of a few 10^{-5} (relative), while the total variation of betatron tunes and magnet strengths are of the order of 10^{-2} (absolute) and 10^{-3} (relative), respectively. These slope values are close to the natural chromaticity values from a design lattice which uses only separate-function magnets $\xi_x \approx$ -9.8 and $\xi_y \approx$ -9.5. The somewhat larger discrepancy between the measurement and simulation in the vertical natural chromaticity is likely the result of employing combined function quadru-sextupoles in the real storage ring which are also used as weak dipole magnets with a large reference orbit displacement in these magnets [36, 37]. In Fig. 2 (e) and (f), the measured tunes are shown as all magnets (both dipoles and quadrupoles/quadru-sextupoles) are varied by the same relative amount (up to 0.2%). The measured tunes remain fairly constant in this range without showing a particular trend, and the resultant small tune variations ($\delta\nu_x \approx 0.0005$, and $\delta\nu_y \approx 0.0007$, peak-to-peak) are at a level expected from various experimental limitations mentioned earlier. This experiment has demonstrated two important results: first, we have independent and accurate control of electron beam energy (using dipoles) and focusing strengths (using quadrupole/quadru-sextupoles); second, the physics idea that scaling the magnetic field in all magnets can reserve tunes (an idea outlined earlier) works rather well in this real storage ring with complicated combined-function magnets.

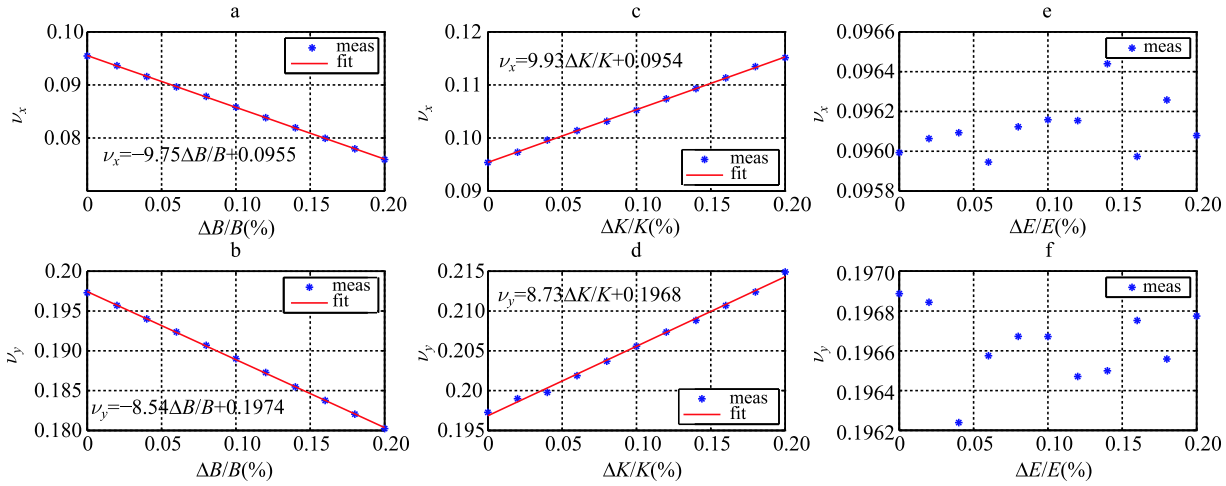

Fig. 2. (color online) Measured betatron tune shifts by scaling the strength of the magnets of different types in the DSR. The measured fractional tunes (ν_x and ν_y) are shown as a function of the change of the relative strength of the magnetic field: subplots (a) and (b) for all dipole magnets, (c) and (d) for all quadru-sextupoles, and (e) and (f) for both dipoles and quadru-sextupoles.

4 Major hysteresis effect

As mentioned in the previous section, by changing the rate of the magnetization process (commonly known as "magnet normalization" in accelerator operation), a magnet can be magnetized to different levels at the end of this process. The amount of time needed to properly complete the magnetization process differs for different types of magnets due to the differences in their size, shape, material used, and the operation range of the field. When the magnetization process is very slow, all major magnets (dipoles, quadrupoles, etc.) will have adequate time to be properly magnetized to reach their expected field values for operation. However, to save the setup time for operation, in practice, a faster magnetization process is commonly used. This may result in some inconsistency between the magnetic fields among dipoles and quadrupoles, leading to noticeable magnetic lattice variations which will show up as betatron tune variations.

In a typical storage ring, lattice preparation is performed to magnetize all major magnets in two steps. First, the currents in these magnets are repeatedly ramped between a set of pre-determined minimum and maximum values for each type of magnets in a so-called magnet normalization cycle. Second, the magnets are ramped toward the final set-points for beam operation (termed "lattice ramping" in this work). Using the DSR, we have investigated these two processes separately using the precision tune measurement system. In this section, we describe our experimental procedures and report our main findings.

For the DSR, all main magnets, including dipoles and quadrupole/quadru-sextupole, were carefully characterized by performing magnetic measurements on each individual magnet. These measurements were used to determine the mappings between the measured magnetic fields and magnet coil currents; these mappings were later implemented in an advanced physics based real-time accelerator control system [38]. For the magnet measurements, the magnet field ramping was usually performed slowly in order to obtain a stable quasi-static magnetization curve. Ideally for acceleration operation, the magnets should be prepared using a ramp rate which is the same as or close to that used in the measurements when possible. However, for practical reasons (e.g. to save time and/or to ramp all types of magnets simultaneously), the magnet normalization for operation is typically carried out at a different rate from that used in the measurements for many storage rings. In the DSR, the ramping rate of a typical normalization cycle is $r_n = r_0 = 10$ MeV/s, and that of lattice ramping is four times slower $r_l = r_0/4 = 2.5$ MeV/s. Both are faster than the typical rate used for magnet measurements $r_{\rm meas} \approx 2$ MeV/s.

To find out the impact of the magnet ramping rates used in the normalization cycle and lattice ramping on the final betatron tunes, three experiments are performed on the DSR by varying the magnet ramping rate in each process. In the first experiment, the rates of normalization cycle and lattice ramping are the same $r_{n,1} = r_{l,1}$ for lattice preparation, and the betatron tunes are measured for the lattices prepared with the ramping rate varied from $r_0/6$ to $4r_0$. In the second experiment, the rate of the normalization cycles is kept constant $r_{n,2} = r_0$ for all the measurements, while the lattice ramping rate is changed in a range. In the third one, the rate of lattice ramping is fixed, but the rate of each normalization cycle is varied. The ramping rates for these experiments are summarized in Table 1.

Table 1. Different ramping rates for magnet normalization (r_n) and lattice ramping (r_l) are used in the three experiments. All ramping rates are expressed in terms of $r_0 = 10$ MeV/s.

experiment	r_n (normalization)	r_l (lattice ramp)
1st Exp	$r_{n,1}$: $r_0/6$ to $4r_0$	$r_{l,1} = r_{n,1}$
2nd Exp	$r_{n,2} = r_0$	$r_{l,2}$: $r_0/4$ to $3r_0$
3rd Exp	$r_{n,3}$: $r_0/2$ to $4r_0$	$r_{l,3} = r_0/4$

To increase the lattice consistency in these experiments, the storage ring lattice is prepared with a proper procedure in which magnets are ramped to 638 MeV settings after three normalization cycles. To reduce the impact of beam current on the measured tunes, the beam current in the storage ring is controlled between 4–4.5 mA and measured tunes are properly corrected to take into account the transverse impedance related tune shift with beam current [39].

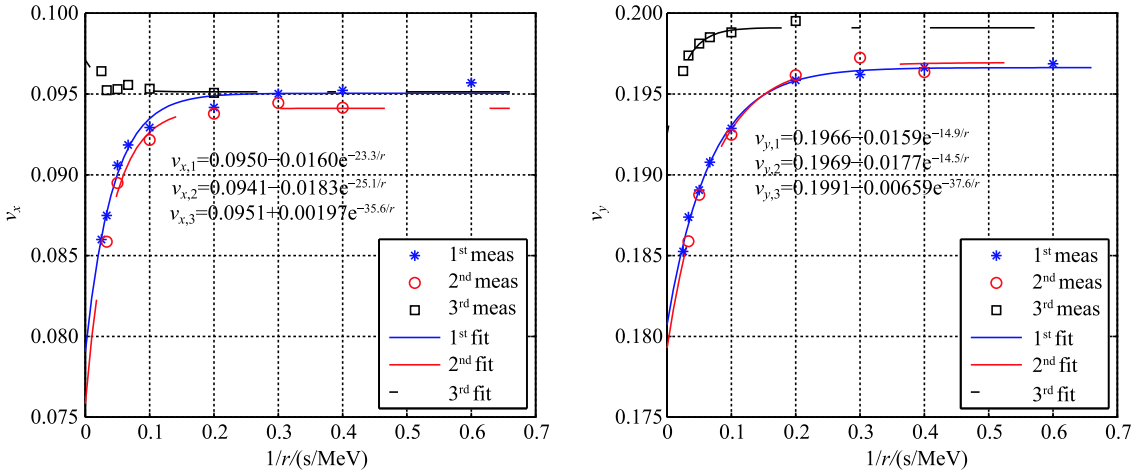

Fig. 3. (color online) Measured fractional betatron tunes of a 638 MeV DSR lattice prepared with different ramping rates used for the lattice setup. The first experiment: $r_{n,1} = r_{l,1}$ and varied together; the second experiment: $r_{n,2} = r_0$ and $r_{l,2}$ is varied; the third experiment: $r_{l,3} = r_0/4$ and $r_{n,3}$ is varied. Three sets of experiments were carried out in three days.

In the first experiment, the magnet ramping rates for normalization and the last step lattice ramping are kept the same, and changed from 1.7 ($r_0/6$) to 40 ($4r_0$) MeV/s. The measured betatron tunes are shown as starred data points in Fig. 3, with each data point representing a complete process of lattice preparation, beam injection, and steady state of storage ring operation for measurements. When the ramping rate is slow enough, roughly $r \leqslant 5$ MeV/s, the measured betatron tunes (both horizontal and vertical) have very consistent values; the measured tunes are found to approach asymptotic values as the ramping rate r approaches zero. This tune behavior can be modeled using an exponential decay as a function of $1/r$, $\nu(r) = \nu_0 + A\mathrm{e}^{-B/r}$, where ν_0 is the asymptotic value, and A and B are two characteristic parameters describing the hysteresis effects (see the inset formulas for $\nu_{x,1}$ and $\nu_{y,1}$ in Fig. 3). The experimental finding of the asymptotic tune values confirms the existence of the stationary hysteresis curve for magnets, which can be approached using a proper normalization procedure at a slow ramping rate.

When the ramping rate is increased from 5 MeV/s to 40 MeV/s, the measured betatron tunes decrease significantly. With faster ramping, the magnet field strength is expected to be slightly smaller than the stationary value, which can cause a tune increase due to weaker dipole magnets (see Section 3) and a tune decrease due to weaker quadrupole magnets. While both effects are present in our experiment, from the observed betatron tune reduction in both directions at a higher ramping rate, we can conclude unambiguously that the quadrupole effect dominates—the loss of the relative quadrupole strength is greater than the loss of the relative dipole strength with fast ramping. A total of about eight hours was used to carry out the first experiment, which involved the study of nine 638 MeV lattices prepared using different ramping rates.

Faster magnet normalization is used in routine operation to save the lattice preparation time. The second experiment is designed to validate this time-saving procedure developed based upon operational experience. In this experiment, the ramping rate for the normalization cycles is fixed at 10 MeV/s ($r_{n,2} = r_0$) the same as in routine operation, while the last step lattice ramping rate $r_{l,2}$ is varied from 2.5 MeV ($r_0/4$) to 30 MeV/s ($3r_0$). The measured betatron tunes (circled data points in Fig. 3) as a function of the ramping rate ($r_{l,2}$) show a very similar trend as in the first experiment, which is easily seen by comparing two sets of fitting curves, $\nu_{x,1}(r)$ vs $\nu_{x,2}(r)$, and $\nu_{y,1}(r)$ vs $\nu_{y,2}(r)$. Again, when $r_{l,2} \leqslant 5$ MeV/s, the measured tune values are reasonably close to their respective asymptotic values, and at a faster rate, a significant tune decrease is observed. Using the fitting model $\nu = \nu_0 + A\mathrm{e}^{-B/r}$, we can make an estimate for the reasonable ramping rate. To achieve a certain tune repeatability $\delta\nu$, the maximum ramping rate is given by $r_{\max} = B/\ln(|A|/\delta\nu)$. In the horizontal direction, a reasonable choice for tune repeatability is $\delta\nu_x = 1\times10^{-4}$, which leads to $r_{1,\max} = 4.6$ MeV/s (exp. #1) and $r_{2,\max} = 4.8$ MeV/s (exp. #2). In the vertical direction, a reasonable choice for tune repeatability is $\delta\nu_y = 2\times10^{-4}$ (the overall focusing in the vertical direction is about one half of that in the horizontal, with $Q_x/Q_y \approx 0.46$, where $Q_{x,y}$ are the total betatron tunes), which leads to $r_{1,\max} = 3.4$ MeV/s (exp. #1) and $r_{2,\max} = 3.2$ MeV/s (exp. #2). These estimated rates confirm that the routine lattice preparation procedure used in operation (10 MeV/s for normalization and 2.5 MeV/s for lattice ramping) is a conservative way to achieve the desirable tune repeatability. In fact, a more general observation can be made: with reasonably fast normalization (in this example, $r_n = 10$ MeV/s), the tune reproducibility is mainly determined by the rate of final lattice ramping.

To explore the possibility of even faster normalization, a third experiment is designed to change the ramping rate for normalization ($r_{n,3}$) while keeping the same slow lattice ramping ($r_{l,3} = 2.5$ MeV/s). The measured tunes are shown as squared data points in Fig. 3. We notice a shift of the vertical tune asymptotic (by about 0.002) which is likely caused by changes of the storage ring operational environment as this experiment was conducted on a different day, including temperature changes, less consistent orbits in the combined function quadrusextupoles, etc. These changes did not impact the overall trend of the measured tunes in the same day, which always showed a high level of consistency (see Fig. 3). Comparing the fitting curves among the three experiments, we notice that in the third experiment, the prefactor coefficient A is much smaller (by a factor of 2.4 to 9.3) and the coefficient in the exponent B is larger (by a factor of 1.4 to 2.6). Furthermore, using the same tune reproducibility criteria, larger maximum ramp rates are found with $r_{\max} = 12$ MeV/s from $\nu_{x,3}(r)$ and 11 MeV/s from $\nu_{y,3}(r)$. In the horizontal direction, when the normalization rate is larger than about 12 MeV/s, the tune is shifted higher as the rate increases, a very surprising finding which indicates the dipole hysteresis effect is now dominating over the quadrupole effect. In addition to reproducing the desired lattice tunes, the lattice preparation is also aimed at producing an electron beam with accurate energy, which requires the hysteresis effect of the dipole magnets to be minimized. Hence it is important not to carry out the normalization cycle too rapidly.

5 Local hysteresis effect

In routine operation or during machine study, the setting of a dipole or a quadrupole/quadru-sextupole is sometimes adjusted by a small amount for compensation or correction. After bringing back the magnet setting, the magnet field seen by the electron beam does not return to the previous value due to local hysteresis, and the discrepancy in the field introduces perturbation to linear and non-linear beam dynamics. In this section, we will present our observations of this type of local hysteresis effect in adjusting quadrupole magnets using a tune based technique, as well as a compensation scheme for this local hysteresis effect, which is very important for characterizing the lattice.

5.1 Beta-function measurement

To characterize a storage ring lattice, a series of direct beta-function measurements can be carried out. A widely used method to directly measure beta-functions of an individually powered quadrupole is to change its focusing strength by a small amount and measure the corresponding betatron tunes. The beta-function averaged for the length of this quadrupole can be expressed as

$$\beta = \frac{2}{\Delta k_1 L_{\rm eff}} \frac{\cos(2\pi\nu_0) - \cos(2\pi\nu')}{\sin(2\pi\nu_0)}, \tag{5}$$

where Δk_1 is the quadrupole strength variation, $L_{\rm eff}$ is the effective length of quadrupole, ν_0 and ν' are the fractional betatron tunes of the unperturbed and perturbed lattices, respectively.

Like most accelerators, the dipoles and quadrupoles in the DSR were fully characterized during the magnetic measurements before installation along the up-curve of the hysteresis loop. The physics-based control system at the DSR can properly set the magnets (dipoles and quadrupoles) along the direction of increasing strength [38]. For example, one can always increase the strength of a quadrupole by changing its setting by Δk_1, positive for a focusing quadrupole and negative for a defocusing quadrupole. After a beta-function measurement, the setting of the quadrupole magnet is usually brought back to the original value to return the lattice back to the original state. However, the focusing strength seen by the electron beams has changed slightly due to local hysteresis in this quadrupole, leading to betatron tune shifts.

An example measurement is taken using focusing quadrupole E04QF in the DSR. In this measurement, the E04QF setting is changed in a local loop of $\Delta\vec{K}_1 = [0, \Delta k_1, 0, -\Delta k_1, 0]$, where Δk_1 is small compared to the nominal quadrupole setting of K_1. The horizontal tune is measured in sequence for each quadrupole setting, and this local loop is repeated 6 times. The beam current dependent tune shift is taken into account so that all measured tune values are properly adjusted for a fixed beam current [39]. To visualize the small shifts along the local loops, a fish-eye plot technique has been developed. The horizontal tune variation with the change of focusing strength setting is shown in Fig. 4, and the related data are collected in Table 2. Given the resolution of the TFB based tune measurement system of about 4×10^{-5}, the non-reproducibility of betatron tunes after completing a local loop can be easily measured.

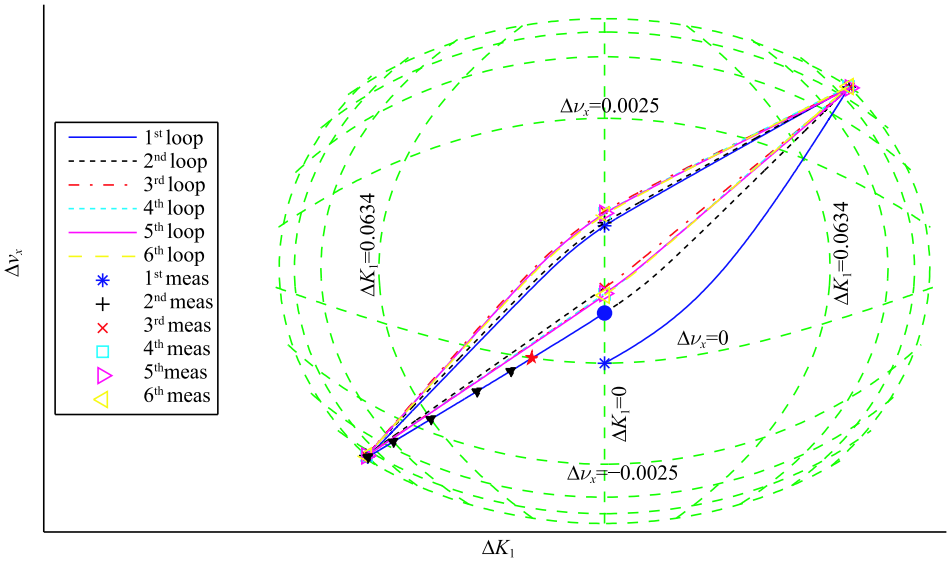

Fig. 4. (color online) Measured horizontal betatron tune variations as the setting of quadrupole E04QF is adjusted in small local loops. The storage ring is operating at 638 MeV. The grid lines are equally spaced with a tune separation $\Delta\nu = 0.0025$ and K_1 separation $\Delta K_1 = 0.0634$ between any two adjacent grids.

Table 2. Measured horizontal betatron tune variations $\Delta\nu_x$ by ramping quadrupole E04QF in local loops.

loop	tune variations $\Delta\nu_x$ $[10^{-3}]$			
$\Delta K_1\left[\frac{1}{m^2}\right]$	0	0.254	0	−0.254
1	0	9.66	1.03	−8.83
2	0.48	9.66	1.06	−8.67
3	0.65	9.62	1.15	−8.70
4	0.61	9.71	1.13	−8.73
5	0.61	9.59	1.13	−8.72
6	0.60	9.71	1.12	−8.72

Equation (5) is employed to calculate the average horizontal beta-function $\beta_{x.i}$ using the two consecutive betatron tunes in each segment of the local loops in sequence, i.e., using the i-th and $(i+1)$th measured betatron tune. The calculated beta-functions are compared with the first measurement $\beta_{x,1}$ (calculated using the 1st and the 2nd tune measurements), which is measured along in the main hysteresis curve and considered to be a "true" beta-function value of the quadrupole, and the relative differences are shown in Fig. 5. As shown in the case of $i=2$, if this quadrupole setting is changed along the reversed direction in the beta-function measurement, the measured beta-function is found to be more than 15% smaller than the true value. However, if the measurement is executed a second time along the up-curve of the hysteresis loop without normalizing this quadrupole magnet (case of $i=5$), an error of about 5% is introduced. Therefore, to measure the beta-function correctly, only betatron tunes measured along the up-curve of the main hysteresis curve should be used. It is also observed in Fig. 4 that the local loops approach a quasi-static limit after repeating the loops a few times, leading to a repetitive pattern in terms of relative beta-function differences shown in Fig. 5. That means a quasi-static minor hysteresis curve can be developed by repeating a specified magnetization cycle. This observation is consistent with practices used to normalize major magnets — the main storage ring magnets are repeatedly ramped between a set of maximum and minimum settings without having to reach "full saturation" and "negative full saturation" (a procedure not practical for accelerators).

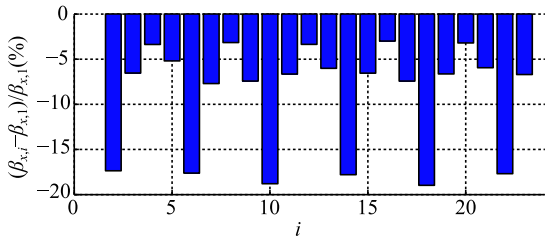

Fig. 5. Relative differences between the first measured beta-function $\beta_{x,1}$ along the up hysteresis curve and additional beta-functions obtained using the tune changes in subsequent segments of the loops. Each loop is separated into four segments, for example, $\beta_{x,2}=2.06$ m is calculated using the second and third betatron tunes measured in the first local loop; $\beta_{x,4}=2.41$ m is calculated using the forth betatron tune measured in the first local loop and the first betatron tune measured in the second loop.

5.2 Local hysteresis compensation

After performing a beta-function measurement in a quadrupole, the setting of the magnet is returned to the original value by completing a closed local loop. However, the small discrepancy of the magnetic field in the quadrupole leads to a small beta beating in the storage ring, which can be estimated using

$$\frac{\Delta\beta(s)}{\beta(s)}=-\frac{2\pi\Delta\nu}{\sin(2\pi\nu_0)}\cos(2\psi(s)-2\psi(s_0)-2\pi\nu_0), \quad (6)$$

where s_0 is the location of the quadrupole, s is an arbitrary location in the storage ring, $\Delta\nu=\nu'-\nu_0$ is the betatron tune shift, and $\Delta\psi=\psi(s)-\psi(s_0)$ is the phase advance between s and s_0. Even though both the tune shift and beta beating caused by one single measurement are small, these effects will accumulate over a series of beta-function measurements. The accumulated effects can become significant to make accurate beta-function measurements impossible. Thus, a local hysteresis compensation scheme is needed.

To precisely restore the storage ring lattice, the quadrupole magnetic field needs to be precisely recovered, which can be verified by checking the return of the betatron tunes. In our experiment with quadrupole E04QF, its final focusing should be set to $\Delta K_1=\Delta k_{1,f}$ (the red star in Fig. 4) to recover the betatron tune rather than to return the quadrupole setting $\Delta K_1=0$ (the blue circle in Fig. 4).

The final quadrupole setting $\Delta k_{1,f}$ can be approached by adjusting the quadrupole strength step by step along the last (or fourth) segment of the first local loop. A typical process to determine $\Delta k_{1,f}$ for a quadrupole in the DSR is as follows. After ramping the quadrupole along a local loop of $\Delta\vec{K}_1=[0,\Delta k_1,0,-\Delta k_1]$ and measuring corresponding betatron tunes $[\nu_0,\nu_1,\nu_2,\nu_3]$, the quadrupole strength is first set to $\Delta K_1=-\Delta k_1/2$ and the corresponding betatron tune ν_4 is measured. By comparing the initial betatron tune ν_0 with ν_4, the next adjustment of the quadrupole strength δk can be estimated using the tune difference $\Delta\nu=\nu_0-\nu_4$ and the slope S between two previous measurements (ν_3 and ν_4) with $\delta k=\Delta\nu/S$. To keep the quadrupole settings along the up hysteresis curve, the final adjustment of the setting is done in multiple steps with decreased step sizes. With a few iterations,

the value of $\Delta k_{1,f}$ is determined when the tune value is within a small range from the original value ν_0 (typically $\delta\nu = 4\times10^{-5}$ or terminated after four iterations), as illustrated by the black solid triangles in Fig. 4. Thus, the special local loop of $\Delta\vec{K}_1 = [0, \Delta k_1, 0, -\Delta k_1, \Delta k_{1,f}]$ is found for a quadrupole to recover the lattice after a beta-function measurement. Due to the local hysteresis, the value of $\Delta k_{1,f}$ for a quadrupole depends on the nominal setting K_1 and the variation step Δk_1 used for the beta-function measurement.

This local hysteresis compensation scheme is developed and utilized in the lattice characterization for the DSR, which employs direct beta-function measurements of all quadrupoles. This scheme works rather well in reducing the accumulated tune shifts, as shown in Fig. 6. In the earlier measurements, the DSR needed to be normalized twice to keep the accumulated tune shifts within 7×10^{-3} in ν_x and 5×10^{-3} in ν_y in the beta-function measurements for all 78 quadrupoles. But with the implementation of the local hysteresis compensation, the tune shifts are reduced to 2×10^{-3} in ν_x and 1×10^{-3} in ν_y without having to normalize the storage ring.

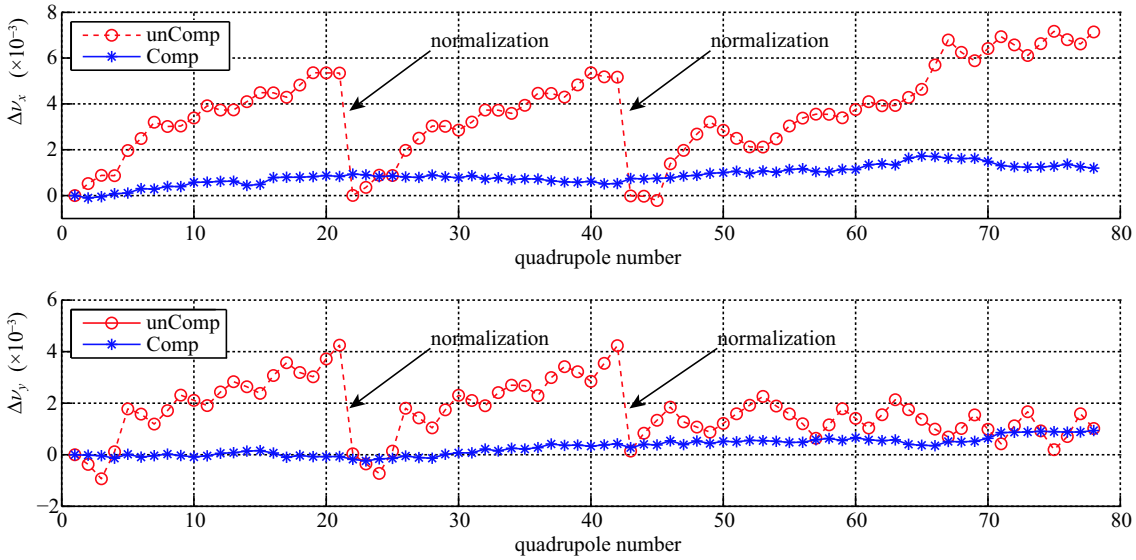

Fig. 6. (color online) Accumulated tune shifts in the lattice characterization for the DSR with a total of 78 quadrupoles. The red circles are tune shifts before performing local hysteresis compensation; two normalization cycles are used to keep the tune shifts in an acceptable range. Blue stars are the accumulated tune shifts with the local hysteresis compensation scheme. The storage ring is operated at 638 MeV.

6 Summary and discussion

In circular accelerators, discrepancies in magnetic fields due to the hysteresis effect in ramping magnets introduce changes to the electron beam energy as well as the storage ring magnetic lattice. Even though the hysteresis effect can be reduced by using proper magnet materials and the lamination technique, it cannot be eliminated completely. This can be a problem for next generation light sources like DLSRs, which require better control of the electron beam parameters and linear/nonlinear dynamics of the electrons. This work is aimed at better understanding the magnet hysteresis effects in storage rings and, furthermore, developing new methods to precisely control the electron beam in operation and machine study.

The main impact of magnet hysteresis has been studied experimentally using the TFB based precision tune measurement system. The first part of this research was carried out to demonstrate independent control of the electron beam energy in the DSR by changing the relative strength of all dipole magnets, as well as independent control of lattice focusing by varying the relative strength of all quadrupole magnets (quadru-sextupoles). Both are useful techniques to measure the natural chromaticity of the storage ring. In the second part of this research, the hysteresis effect associated with the normalization cycles and lattice ramping in the process of lattice preparation has been studied in detail using a series of measurements with three different ways to vary the magnet ramping rates. Our experimental results show that the rate for the normalization cycles can be increased to a certain level to save the lattice preparation time, and good betatron tune reproducibility can be realized with relatively slow final lattice ramping toward the operation set-point. Based upon the experimental results, we have

provided a way to estimate the maximum ramping rates for both normalization cycles and lattice ramping.

To understand the local hysteresis effect, we have studied the tune shifts due to focusing strength discrepancy resulting from quadrupole adjustments in the beta-function measurement. Observation in this experiment suggests that the beta-function should be measured along the up-curve of the main hysteresis loop. It also indicates that a quasi-state local hysteresis loop can be approached by repeating a special local magnetization routine in the magnet. A local hysteresis compensation scheme has been carefully developed to closely recover lattice focusing by bringing back the betatron tunes after a beta-function measurement. With the application of this scheme in the lattice characterization for the DSR, the accumulated betatron tune shifts are significantly reduced without having to normalize the storage ring magnets during the process of measuring the beta-functions for all 78 quadrupoles.

We would like to thank the engineering and technical staff at DFELL/TUNL for their support of this research work. One of the authors (Wei Li) also would like to thank the China Scholarship Council (CSC) for supporting his research visit at Duke University.

References

1 M. Eriksson et al, J. Synchrotron Rad., **21**: 837 (2014)
2 D. Einfeld et al, J. Synchrotron Rad., **21**: 856 (2014)
3 J. Chavanne et al, Synchrotron Rad. News, **28**: 15 (2015)
4 P. F. Tavares et al, J. Synchrotron Rad., **21**: 862 (2014)
5 W. Fan et al, Sci. Chin. Phys. Mechanics and Astronomy, **55**: 802 (2012)
6 U. Bergmann et al, *Science and technology of future light sources: A white paper*, No. SLAC-R-917, Stanford Linear Accelerator Center (SLAC) (2009)
7 E. Al-Dmour et al, J. Synchrotron Rad., **21**: 878 (2014)
8 M. Hettel et al, Perspectives and Challenges for Diffraction-Limited Storage Ring Light Sources. Proc. NA-PAC13 (2013)
9 J. C. Chang et al, Numerical Simulation and Air Conditioning System Study for the Storage Ring of TLS, Proc. IPAC, (2010)
10 D. P. Barber et al, Phys. Lett. B, **135**: 498 (1984)
11 A. S. Artamonov et al, Phys. Lett. B, **118**: 225 (1982)
12 K. Chouffani et al, Phys. Rev. ST- A&B, **9**: 050701 (2006)
13 V. E. Blinov et al, Nucl. Instrum. Methods A, **494**: 81 (2002)
14 C. Sun et al, Phys. Rev. ST-A&B, **12**(6): 062801 (2009)
15 W. Xu et al, Chin. Phys. C, **37**:76 (2013)
16 P. Langevin, J. Phys, **4**: 678 (1905)
17 P. Langevin, Annales de Chimie et de Physique, **5**: 70 (1905)
18 M. Rao et al, Phys. Rev. B, **42**: 856 (1990)
19 M. Rao et al, Phys. Rev. B, **43**: 3373 (1991)
20 D. Dhar et al, J. Phys. A: Mathematical and General, **25**: 4967 (1992)
21 I.D. Mayergoyz, *Mathematical models of hysteresis* (New York: Springer-Verlag, 1991)
22 B. D. Coleman et al, Arch. Rat. Mech. Analys., **99**: 375 (1987)
23 B. D. Coleman et al, Int. J. Eng. Sci., **24**: 897 (1986)
24 D. C. Jiles et al, IEEE Trans. Magn., **19**: 2183 (1983)
25 D. C. Jiles et al, J. Appl. Phys., **55**: 2115 (1984)
26 D. C. Jiles et al, J. Magn. Magn. Mater., **61**: 48 (1986)
27 D. C. Jiles et al, J. Magn. Magn. Mater., **92**: 289 (1990)
28 D. C. Jiles, IEEE Trans. Magn., **28**: 2602 (1992)
29 D. C. Jiles, IEEE Trans. Magn., **29**: 3490 (1993)
30 D. C. Jiles, J. Appl. Phys. **76**: 5849 (1994)
31 J. A. Ewing et al, *Magnetic Qualities of Iron*, Proc. R. Soc. London, **54**: 75-77 (1893)
32 M. L. Hodgdon, IEEE Trans. Magn., **24**:3120 (1988)
33 D. C. Jiles et al, IEEE Trans. Magn., **25**: 3928 (1989)
34 S. Y. Lee, *Accelerator physics* (Singapore: World scientific, 1999)
35 Y. K. Wu, *Theoretical and experimental studies of the beam physics in the duke fel storage ring*, Ph.D Thesis (1995)
36 J.T. Tanabe, *Iron dominated electromagnets: design, fabrication, assembly and measurements* (World Scientific, 2005)
37 V. N. Litvinenko et al, Performance of Achromatic Lattice with Combined Function Sextupoles at Duke Storage Ring, Proc. PAC, **2**:796 (1995)
38 Y. K. Wu et al, A Physics Based Control System for the Duke Storage Ring, Proc. PAC, **4**: 2483 (2003)
39 A. Chao et al, Phys. Rev. ST-A&B, **5**: 111001 (2002)